EPB41L5 functions to post-transcriptionally regulate cadherin and integrin during epithelial–mesenchymal transition

Mariko Hirano,[1,4] Shigeru Hashimoto,[4] Shigenobu Yonemura,[3] Hisataka Sabe,[4] and Shinichi Aizawa[1,2]

[1]Laboratory for Vertebrate Body Plan, [2]for Animal Resources and Genetic Engineering, and [3]for Cellular Morphogenesis, Center for Developmental Biology (CDB), RIKEN Kobe, Chuo-ku, Kobe 650-0047, Japan
[4]Department of Molecular Biology, Osaka Bioscience Institute, Suita-shi, Osaka 565-0874, Japan

EPB41L5 belongs to the band 4.1 superfamily. We investigate here the involvement of EPB41L5 in epithelial–mesenchymal transition (EMT) during mouse gastrulation. EPB41L5 expression is induced during TGFβ-stimulated EMT, whereas silencing of EPB41L5 by siRNA inhibits this transition. In EPB41L5 mutants, cell–cell adhesion is enhanced, and EMT is greatly impaired during gastrulation. Moreover, cell attachment, spreading, and mobility are greatly reduced by EPB41L5 deficiency. Gene transcription regulation during EMT occurs normally at the mRNA level; EPB41L5 siRNA does not affect either the decrease in E-cadherin or the increase in integrin expression. However, at the protein level, the decrease in E-cadherin and increase in integrin are inhibited in both EPB41L5 siRNA-treated NMuMG cells and mutant mesoderm. We find that EPB41L5 binds p120ctn through its N-terminal FERM domain, inhibiting p120ctn–E-cadherin binding. EPB41L5 overexpression causes E-cadherin relocalization into Rab5-positive vesicles in epithelial cells. At the same time, EPB41L5 binds to paxillin through its C terminus, enhancing integrin/paxillin association, thereby stimulating focal adhesion formation.

Introduction

Animals use a succession of tissue transformations between epithelium and mesenchyme to achieve tissue remodeling during embryogenesis. Upon transdifferentiation of epithelial cells to mesenchymal cells (epithelial–mesenchymal transition [EMT]), cells detach from neighboring cells and acquire migratory potential. Mesoderm and endoderm cells are formed during gastrulation with EMT of embryonic ectoderm or epiblast cells. A number of genes are known to be either down- or up-regulated at the transcriptional level (Yamaguchi et al., 1994; Sun et al., 1999; Batlle et al., 2000; Cano et al., 2000; Carver et al., 2001; Lee et al., 2006). At the same time, it is believed that post-transcriptional events must also play crucial roles in the EMT (Xue et al., 2001; Zohn et al., 2006), although the details of such events are still largely unknown.

The principal mediator of cell–cell adhesion in the epithelial cell sheet is the cadherin-mediated adherens junction specialized at subapical surfaces (D'Souza-Schorey, 2005). Focal adhesions are the extracellular matrix (ECM)–integrin junctions that bring together cytoskeletal and signaling proteins during the process of cell spreading and migration (Mitra et al., 2005). Upon EMT the disassembly of the adherens junctions correlates with a loss of cell–cell contact and an acquisition of migratory potential by the activation of focal adhesions; the two processes must be tightly coordinated. Dynamics of the adherens junctions and focal adhesions are controlled by the assembly and disassembly of adhesion components coupled with cytoskeletal remodeling. It has been suggested that p120 catenin (p120ctn) regulates the stability of E-cadherin in adherens junctions (Ireton et al., 2002; Davis et al., 2003; Peifer and Yap, 2003; Xiao et al., 2007). Paxillin is a key factor regulating focal adhesion dynamics (Kondo et al., 2000; Hagel et al., 2002).

Band 4.1 superfamily members have a FERM domain at their N terminus and an actin-binding domain at their C terminus, and are thought to play crucial roles in the regulation of interactions between integral plasma membrane proteins and cytoskeleton just beneath the plasma membrane (Sun et al., 2002). By the

Correspondence to Shinichi Aizawa: saizawa@cdb.riken.jp

Abbreviations used in this paper: Crb, Crumbs; EMT, epithelial–mesenchymal transition; p120ctn, p120 catenin.

The online version of this article contains supplemental material.

The Rockefeller University Press $30.00
J. Cell Biol. Vol. 182 No. 6 1217–1230
www.jcb.org/cgi/doi/10.1083/jcb.200712086

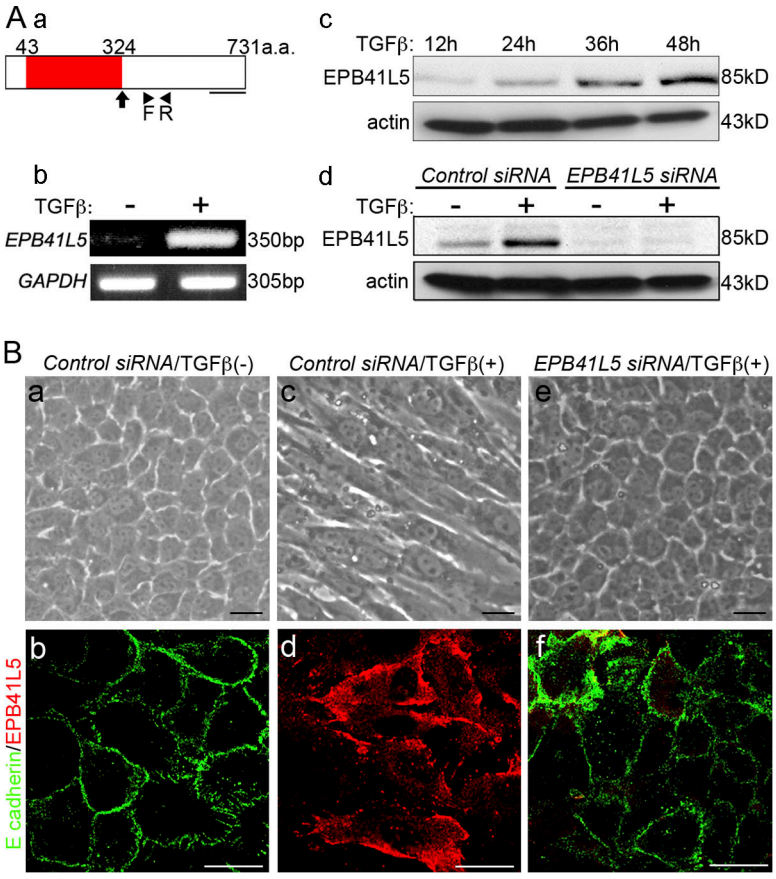

Figure 1. **EPB41L5 functions in EMT of NMuMG cells by TGFβ.** (A) EPB41L5 expression in NMuMG cells. (a) Schematic representation of EPB41L5. Red represents FERM domain. An arrow indicates the point of truncation in the analyses of Fig. 6 (d–f), Fig. 7 (e–l), Fig. 8 (d), and Fig. 9 (Bc and d). The underline indicates the location of the sequences used as an antigen to raise an antibody. Arrowheads (F, R) indicate the locations of primers for RT-PCR analyses in b. (b and c) The increase in EPB41L5 expression with the TGFβ treatment assayed by RT-PCR (b) at 48 h and Western blotting (c) at the indicated time. (d) Effect of *EPB41L5* siRNA treatment on the EPB41L5 protein induction by TGFβ. The cells were transfected with control or *EPB41L5* siRNA and cultured in the absence or presence of TGFβ for 48 h. (B) Inhibition of TGFβ-induced EMT of NMuMG cells by *EPB41L5* siRNA. EPB41L5 (red) is scarce in the confluent epithelial NMuMG cells in the absence of TGFβ; E-cadherin (green) is abundant at cell–cell contact sites (a and b). In "mesenchymal" cells induced by TGFβ, EPB41L5 is abundantly present with no E-cadherin expression (c and d). *EPB41L5* siRNA inhibits the transformation into "mesenchyme" by TGFβ (e), retaining E-cadherin at cell–cell contact sites (f). Bars, 20 μm.

presence and absence of characteristic domains at the C-terminal side they are classified into several families: Band 4.1, PTPH, ERM, talin, and novel band 4.1 like (NB41L) families. The NB41L family has unique nonhomologous C termini and lacks an actin-binding domain; the family can be further divided into EPB41L4a and EPB41L5 families by the sequence identity of the FERM domain. In the mouse, the EPB41L5 family includes another member, EPB41L4b/Ehm2, in addition to the EPB41L5 examined in this study; all vertebrates have two members in the EPB41L5 family, whereas *Drosophila* has only one. *Drosophila* Yurt and zebrafish Moe in this family have recently been demonstrated to function as negative regulators of Crumbs (Crb) orthologues, which control epithelial polarity and apical membrane size in embryonic epithelia and photoreceptor cells (Jensen and Westerfield, 2004; Hsu et al., 2006; Laprise et al., 2006).

In this study we demonstrate that mouse EPB41L5 plays essential roles in EMT and cell migration during mouse gastrulation. We propose that EPB41L5 coordinates the down-regulation of E-cadherin–mediated cell–cell adhesion and activation of integrin-mediated cell–ECM adhesion in a post-transcriptional manner during EMT. EPB41L5 may destabilize E-cadherin by binding to p120ctn, predisposing it toward endocytosis. EPB41L5 also binds to paxillin and enhances paxillin/integrin association, thereby activating focal adhesions. The study reveals a new aspect of the function of scaffold band 4.1 superfamily member proteins, which is obviously different from its function as a component of the Crumbs complex, but consistent with the *EPB41L5* activation in oncogenic cells.

Results

EPB41L5 in EMT of NMuMG cells

Erythrocyte band 4.1 superfamily proteins have been suggested to play roles in epithelial integrity, and we had chosen epithelial NMuMG cells to examine EPB41L5 functions. However, EPB41L5 was barely detectable in confluent epithelial NMuMG cells (Fig. 1, Ab, c, and Bb). Epithelial NMuMG cells are transformed into mesenchyme-like cells ("mesenchyme") by treatment with TGFβ (Miettinen et al., 1994). With this transition, the EPB41L5 expression was markedly elevated (Fig. 1, Ab, c, and Bd). In addition, *EPB41L5* siRNA inhibited the EMT of NMuMG cells by TGFβ. At the mRNA level, even when the EPB41L5 protein expression was inhibited by the siRNA (Fig. 1 Ad), *E-cadherin* expression was reduced and *β1-integrin*, *Snail*, and *Twist* expression were all enhanced normally by TGFβ (Fig. 2, Aa and Ba). At the protein level, however, E-cadherin expression was retained and β1-integrin expression was not elevated significantly (Fig. 2, Ab and Bb). *EPB41L5* siRNA did not affect the increase in N-cadherin expression by TGFβ; nor did it affect α-catenin, β-catenin, p120ctn, or paxillin expression (Fig. 2 A). Concomitantly, *EPB41L5* siRNA-treated NMuMG cells did not undergo morphological transformation into "mesenchyme" by TGFβ, retaining E-cadherin at the sites of cell–cell contact (Fig. 1, Be and f).

Mesodermal defects in *EPB41L5* mutants

To confirm *EPB41L5* functions in the EMT in vivo, we next generated a mouse mutant (Fig. S1 A, available at

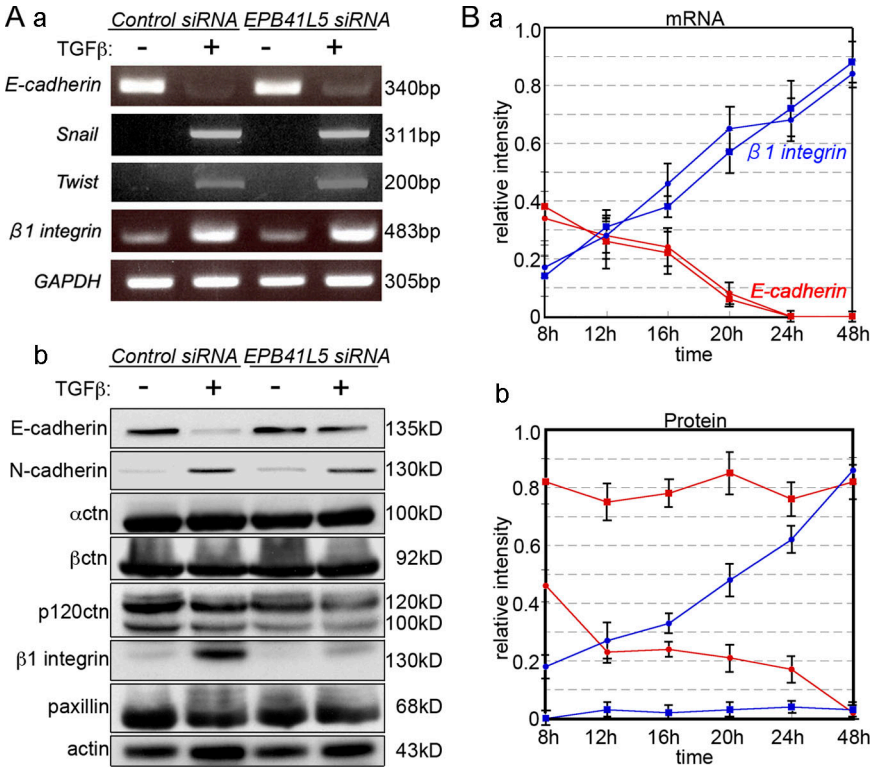

Figure 2. **Changes in E-cadherin and β1-integrin expression by TGFβ and/or *EPB41L5* siRNA treatment of NMuMG cells.** (A) RT-PCR (a) and Western blot (b) analysis. Cells transfected with control or *EPB41L5* siRNA were plated at $10^4/cm^2$ and cultured in the absence (−) or presence (+) of TGFβ for 48 h, and the expression of each molecule indicated was determined. (B) Quantitation of E-cadherin (red lines) and β1-integrin (blue lines) expression by RT-PCR (a) and Western blotting (b) at the indicated time after plating. Circles represent the cells transfected with control siRNA, and squares those with *EPB41L5* siRNA. Ordinates give the relative intensity to *GAPDH* (a) or actin (b) expression, respectively, determined with ImageJ software. The experiment was repeated three times.

http://www.jcb.org/cgi/content/full/jcb.200712086/DC1). The mutant is null as demonstrated by RT-PCR analysis with primers at the site of mutation and at the 3′ exons and by Western blot analysis (Fig. S1, Bc and d).

During gastrulation EPB41L5 protein was apparent at the cell periphery in invaginating cells (Fig. S2 Bc, available at http://www.jcb.org/cgi/content/full/jcb.200712086/DC1). In ectoderm, EPB41L5 was enriched at both the apical and basal sides, but less abundant on lateral sides (Fig. S2 Bd); details of EPB41L5 expression in early embryogenesis are given in Fig. S2. At E6.5 mutant embryos were proximo-distally reduced in size but histologically almost normal (Fig. S2, Ca and a'; Fig. 3, Aa and b). At E7.5 the embryos were hypomorphic (Fig. S2, Cb and b'); spaces were scarce among three germ layers, and embryonic cells in each layer appeared to be stacked together (Fig. 3, Ab and b'). *Snail*-positive mesoderm cells were differentiating, but they spread poorly over the embryos (Fig. 3, Ba and a'). *Brachyury*-positive axial mesoderm developed in the primitive streak, but did not extend anteriorly beyond the node (Fig. 3, Bb and b'). At E8.5 the rostro-caudal extension was retarded in the mutants (Fig. S2, Cc and c'), and development of headfold was meager with minimum mesoderm cells (Fig. 3, Ac and c'). The foregut failed to close and neuroectoderm was hypertrophic (Fig. S2, Da, a', c, and c'); E8.5 wild-type anterior neuroectoderm was still a single cell layer of the epithelial plate (Fig. S2 Dd), whereas in *EPB41L5* mutants the neural plate was multi-cell layered (Fig. S2 Dd'). Presomitic mesoderm was generated but segmented somites were never formed in the mutants (Fig. 3, Ac and c'; Fig. S2, Db and b'). Marker analyses confirmed these mesodermal defects (Fig. S3 A, available at http://www.jcb.org/cgi/content/full/jcb.200712086/DC1), but the mutant developed cells in each germ layer and anterior–posterior pattern normally (Fig. S3). These mutant phenotypes are essentially the same as those of an ENU-induced mutant, *limulus* (*lulu*), recently reported (Lee et al., 2007); it has a point mutation at the 5′ terminus of *EPB41L5* coding region, generating a stop codon or a null mutation.

EPB41L5 mutant defects in EMT during gastrulation

Under electron microscopy, defects were also not apparent at E6.5, with the exception of several invaginating mesoderm cells in tight contact (Fig. 3, Ca–b'). Laterally, several invaginated cells were also attached tightly to each other (Fig. 3 Cc'). Cell architecture was mostly normal in epiblast and endoderm. At E7.5 defects were apparent over three germ layers. Ectoderm cells lost their columnar epithelial shape and were multilayered; they were associated closely with minimal intercellular spaces (Fig. 3, Cd and d'; see also Fig. 4 c'). Tight junction, adherens junction, and desmosome were normally formed in the most apical layer of the cells (Fig. 3, Ce and e'), but not in other cells. ZO-1 and occludin, components of the tight junction, were also found as normal in the most apical layer of *EPB41L5* mutant ectoderm (not depicted). Basement membrane was barely detectable in the basal side of ectoderm cells in any layers (Fig. 3, Cf and f'). Collagen type IV and laminin, components of the basement membrane, were partially present beneath the multilayered ectoderm cells (Fig. 4).

Increase of cell number in ectoderm with multi-cell stratification would be explained by increase in cell proliferation or decrease in cell apoptosis. However, the ratio of BrdU incorporating cells was 24.8% in wild-type and 25.2% in mutant ectoderm

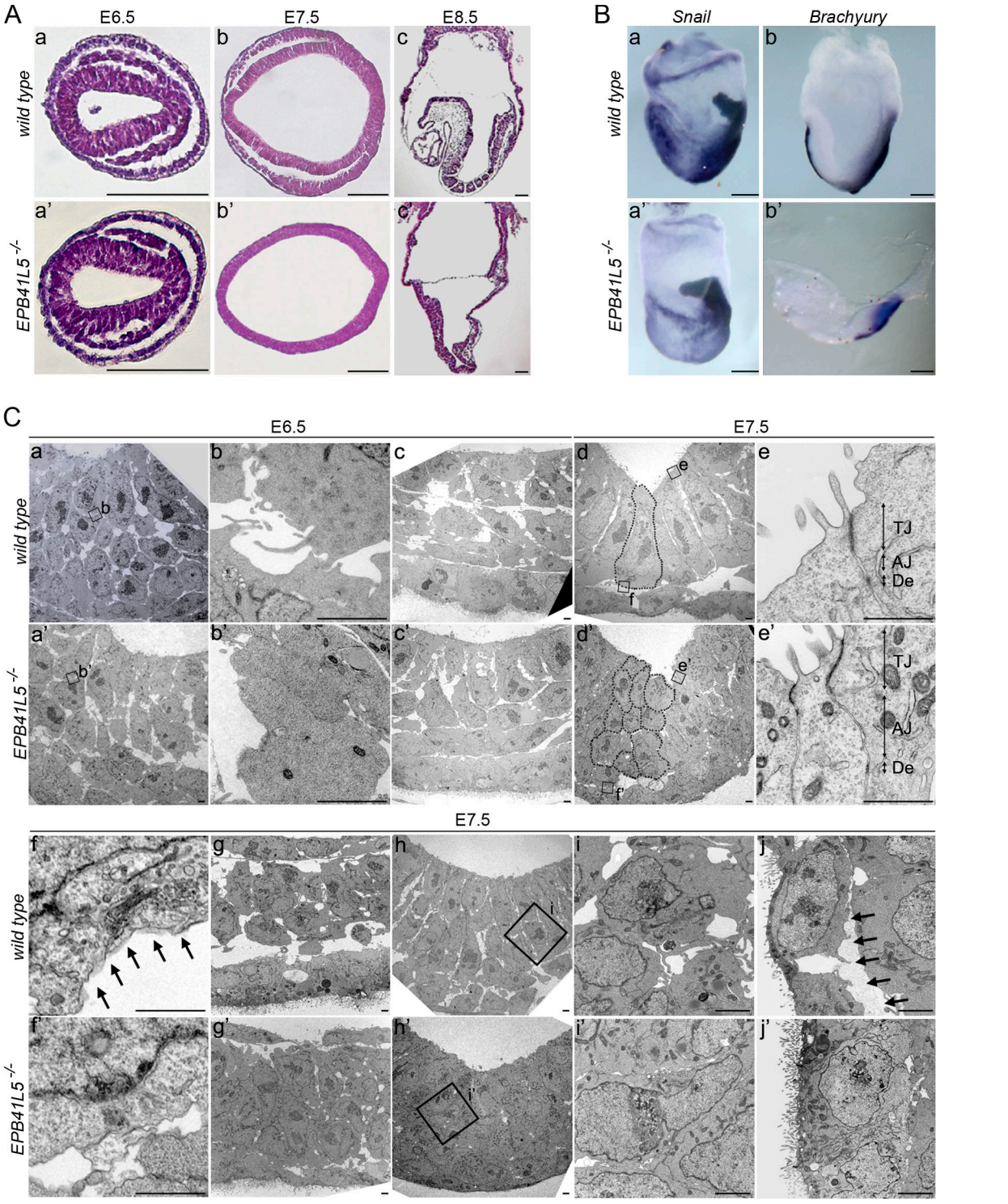

Figure 3. ***EPB41L5* mutant phenotype.** (A) Histological views of wild-type (a–c) and mutant (a′–c′) embryos at E6.5 (a and a′), E7.5 (b and b′), and E8.5 (c and c′), respectively. (a, a′, b, and b′) Horizontal sections. (c and c′) Sagittal sections. Anterior is to the left. Bars, 100 µm. (B) Whole-mount RNA in situ hybridization views of wild-type (a and b) and mutant (a′ and b′) embryos at E7.5 for *Snail* (a and a′) and *Brachury* (b and b′) expression. Lateral views; anterior is to the left. Bars, 100 µm. (C) Electron microscopic views of *EPB41L5* mutant embryos. (a–j) Views in wild-type. (a′–j′) Views in *EPB41L5* mutant embryos. (a and a′) Views at E6.5 primitive streak. (b and b′) Enlarged views of the regions boxed in a and a′, respectively. (c and c′) Views of the lateral region of E6.5 embryos. (d and d′) Views of the anterior region of E7.5 embryos. (e–f′) Enlarged views of the regions boxed in d and d′. (g and g′) Views of laterally invaginated E7.5 mesoderm cells. (h and h′) Views of cells invaginating at E7.5 primitive streak. (I and i′) Enlarged views of the regions boxed in (h and h′). (j and j′) Views of E7.5 endoderm cells. Dotted lines in d and d′ outline individual cells in the anterior-most ectoderm layers; these cells are ectodermal, as suggested by the location of residual basement membrane components and E-cadherin expression shown in Fig. 4, b′ and c′. Arrows in f and j indicate basement membranes. In e and e′, TJ is tight junction; AJ, adherens junction; De, desmosome. Bars, 5 µm.

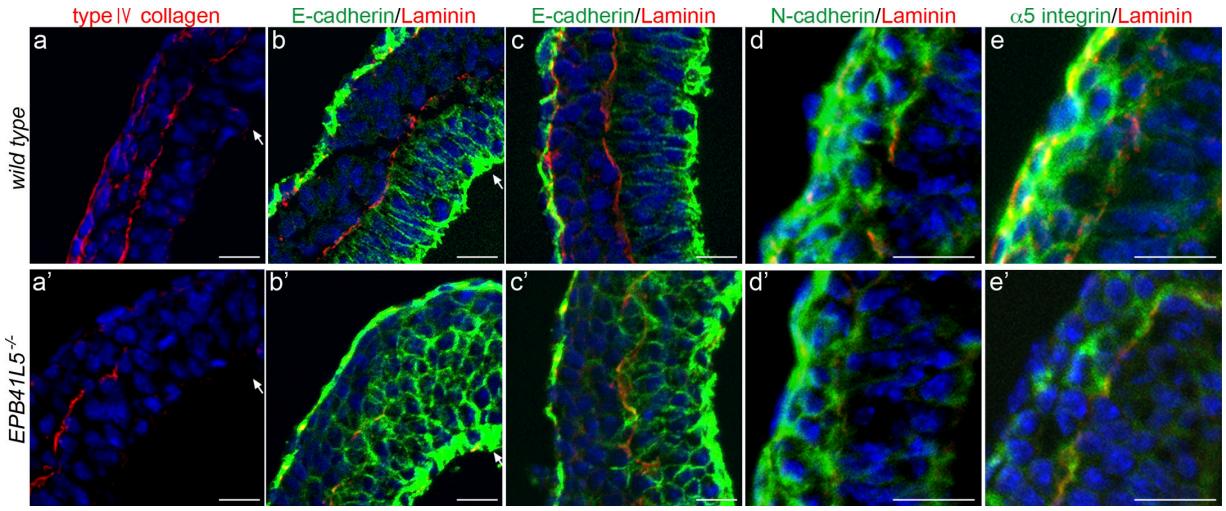

Figure 4. **Marker analyses of epithelial mesenchyme transition in *EPB41L5* mutant gastrula.** (a–e) Wild-type and (a′–e′) mutant embryos at E7.5. Red indicates type IV collagen staining in a and a′ and laminin staining in b–e′ for basement membranes, and blue DAPI staining for nucleus in all figures. (b–c′) E-cadherin staining (green) at the primitive streak region (b and b′) and lateral region (c and c′). (d and d′) N-cadherin. (e and e′) α5-integrin staining (green). Arrows indicate invagination sites. (c′) Ectodermal nature of the multi-layered cells by the locations of residual laminin-positive basement membranes and E-cadherin expression (compare Fig. 3 Cd′). Bars, 20 μm.

under the conditions examined, and no difference was apparent in the frequency of TUNEL-positive cells (unpublished data). Moreover, the total cell number was around 15,000 per embryo in both wild-type and mutant E7.5 embryos.

At E7.5 a significant number of mesoderm cells are present in the anterior part of wild-type embryos. However, they were few in *EPB41L5* mutant embryos. Laterally intercellular space was scarce among invaginated mesoderm cells, and the cells adhered tightly to each other (Fig. 3, Cg and g'). Most prominently, at the primitive streak invaginating cells were in tight contact with little intercellular space (Fig. 3, Ch–i'). Endoderm cells also adhered tightly, and basement membrane was not found electron microscopically (Fig. 3, Cj and j'); collagen type IV or laminin was also not apparent in the endoderm layer (Fig. 4). Intercellular space was scarce not only between adjacent cells in each germ layer but also among cells in the three germ layers.

In wild-type embryos, ectoderm and endoderm cells express E-cadherin (Fig. 4, b and c); this expression decreases in invaginating mesodermal cells (Fig. 4 b) and is lost in invaginated cells (Fig. 4 c), acquiring N-cadherin (Fig. 4 d) and α5-integrin (Fig. 4 e) expression. In *EPB41L5* mutants, E-cadherin not only continued to be expressed in invaginating mesoderm cells but also persisted in invaginated mesoderm cells (Fig. 4, b' and c'). N-cadherin expression took place apparently normally while α5-integrin expression did not in the mutant invaginated mesodermal cells (Fig. 4, d' and e'). Thus, the decrease in E-cadherin expression and the increase in integrin expression during cell invagination are inhibited, but the increase in N-cadherin expression is not, by the *EPB41L5* deficiency. These are consistent with the observations in NMuMG cells (Fig. 2).

EPB41L5 in cell–cell and cell–substrate adhesions

The increase in cell–cell adhesion by *EPB41L5* deficiency was also demonstrated in vitro by the aggregation assay with mutant embryonic cells (unpublished data). It was also demonstrated with TGFβ-treated NMuMG cells by the *EPB41L5* siRNA treatment (Fig. 5 A). Thus, the defects in the mesoderm transition and mesoderm movement by *EPB41L5* deficiency could be ascribed to the retention of E-cadherin–mediated cell–cell interaction (Fig. 4, b' and c'), as is the case in p38-deficent embryos (Zohn et al., 2006). The effect of cell surface E-cadherin down-regulation on cell movement of *EPB41L5* mutant primitive streak cells was then examined with anti–E-cadherin antibody. However, the antibody treatment was not sufficient to restore cell movement of *EPB41L5* mutant primitive streak cells (Fig. 5 B), suggesting that cell–ECM interaction is also affected in the mutant.

Indeed, E7.5 *EPB41L5* mutant embryonic cells were found to attach poorly to a fibronectin-coated dish; about half of the cells did not attach even after overnight culture (Fig. 5 Ca), and their spreading was also poor (unpublished data). The decrease in cell attachment to fibronectin-coated dish was also demonstrated with NIH3T3 and TGFβ-treated NMuMG cells by *EPB41L5* siRNA treatment (Fig. 5 Cb; Fig. S4 Aa, available at http://www.jcb.org/cgi/content/full/jcb.200712086/DC1); cell spreading was also reduced by this treatment (Fig. 5, Cc and d; Fig. S4, b and c).

Next, the decrease in mobility of *EPB41L5* mutant embryonic cells was demonstrated by time-lapse cinematography (unpublished data). It was also observed with NIH3T3 and TGFβ-treated NMuMG cells after siRNA treatment (Fig. 5 D; Fig. S4 B). Furthermore, wound healing was also impaired by *EPB41L5* siRNA. When monolayer NIH3T3 or TGFβ-treated NMuMG cells are scratched and cultured, the scratch is normally restored by cell migration (Fig. 5 Ea; Fig. S4 Ca). This recovery was greatly impaired when the cells were treated with *EPB41L5* siRNA (Fig. 5 Eb, Fig. S4 Cb). Thus, not only cell–cell adhesions are enhanced, but also cell adhesions to substrate are impaired by *EPB41L5* deficiency.

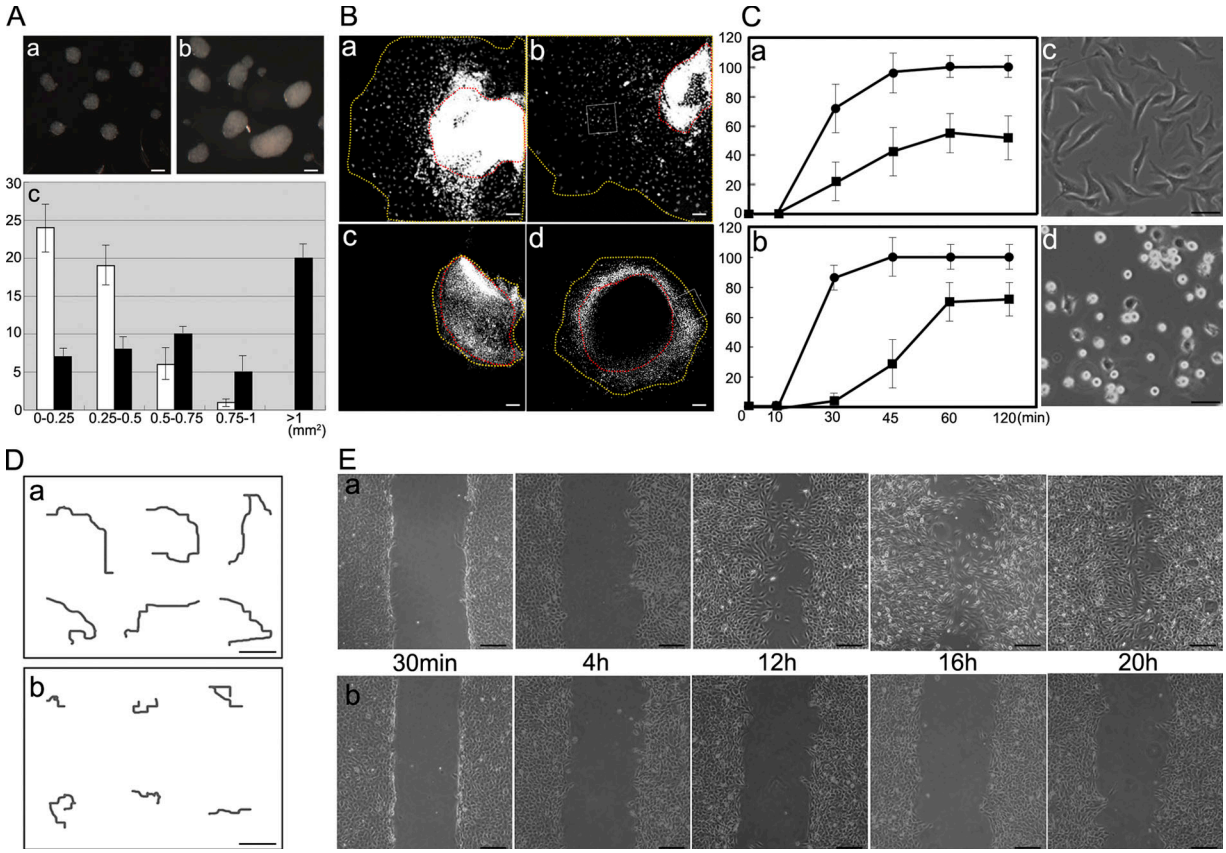

Figure 5. **Roles of EPB41L5 in cell–cell and cell–substrate interaction.** (A) Cell aggregation assay. NMuMG cells were treated with TGFβ for 48 h and transfected with (a) control or (b) *EPB41L5* siRNA. After 12 h, cells were trypsinized and cultured in suspension for 4 h as described previously (Takeichi, 1977). (a and b) Examples of cell aggregates. (c) Size distribution of the aggregates; the size is represented as the product of the major and minor axes. 50 aggregates were counted, and their frequency in the size range indicated at the abscissa is given in the ordinate for control (white columns) and *EPB41L5* (black columns) siRNA-treated cells. Bars, 200 µm. (B) Effects of anti–E-cadherin antibody on mobility of *EPB41L5* mutant primitive streak cells. Primitive streak was dissected from wild-type (a and b) or mutant (c and d) E7.5 embryos and cultured with control DMSO (a and c) or rat anti–mouse E-cadherin antibody (b and d) for 2 d as described previously (Zohn et al., 2006). Red lines indicate the peripheries of primitive streak cell mass and yellow lines the forefront of migrating cells. See Fig. 9 D for the boxes in b and d. Bars, 200 µm. (C) Cell attachment assay to fibronectin-coated substrates. (a) The assay with wild-type (●) and *EPB41L5* mutant (■) cells dispersed by trypsinization and pipetting from E7.5 whole embryos; (b), the assay with NIH3T3 cells transfected with control (●) or *EPB41L5* (■) siRNA. (c and d) Spreading of NIH3T3 cells transfected with control (c) or *EPB41L5* (d) siRNA after 120 min culture. NIH3T3 cells express EPB41L5 at the comparable level to that in TGFβ-treated NMuMG cells shown in Fig. 1 A. Bars, 100 µm. (D) Cell movement on the fibronectin-coated substrates. NIH3T3 cells transfected with control (a) or *EPB41L5* (b) siRNA were plated sparsely, and after 8 h the movement of individual cells was traced by time-lapse cinematography for 12 h. Typical examples of the tracing are shown on six cells, respectively. Bars, 100 µm. (E) Wound-healing assay on the fibronectin-coated substrates. (a and b) NIH3T3 cells transfected with control (a) or *EPB41L5* (b) siRNA were plated at a high cell density, and the monolayers were scratched 12 h after plating and cultured for the indicated times. Bars, 200 µm. Similar observations on cell attachment, spreading, and mobility obtained with TGFβ-treated NMuM G cells are presented in Fig. S4.

EPB41L5 interaction with E-cadherin–associated adhesion components

E-cadherin degradation is known to be mediated by Arf6, Hakai, and p120ctn (D'Souza-Schorey, 2005; Xiao et al., 2007). EPB41L5 bound to p120ctn, but not to Arf6 or Hakai (Fig. 6 a). Moreover, in TGFβ-treated NMuMG cells endogenous EPB41L5 was found to associate with p120ctn (Fig. 6 b). EPB41L5 did not bind to either α- or β-catenin. p120ctn that lacked an N terminus could associate with EPB41L5, but that which lacked a C terminus could not (Fig. 6 c). The C-terminal region of p120ctn consists of armadillo repeats and a tail domain; deletion of the tail domain did not affect the binding to EPB41L5 (unpublished data). On the other hand, although EPB41L5 lacking the C terminus (EPB41L5ΔC) could associate with p120ctn, that lacking the N terminus (EPB41L5ΔN) could not (Fig. 6 d). Thus, these two proteins probably interact through armadillo repeats of p120ctn and FERM domain of EPB41L5. p120ctn binds to E-cadherin also through armadillo repeats. The effects of EPB41L5 on E-cadherin–p120ctn interaction were therefore examined. p120ctn binding to E-cadherin was indeed inhibited by EPB41L5, but not by EPB41L5 lacking the N terminus (Fig. 6 e). EPB41L5 lacking C-terminal but having N-terminal FERM domain (EPB41L5ΔC) also inhibited p120ctn binding to E-cadherin (Fig. 6 f). p120ctn also binds to N-cadherin, but this binding was not affected by EPB41L5 (Fig. 6 g). Wild-type EPB41L5 and EPB41L5 lacking C-terminal with intact N-terminal FERM domain localized at the cell membrane, but EPB41L5 lacking the N-terminal did not (Fig. 7, b, f, and j; Fig. 9 B; Fig. S5, available at http://www.jcb.org/cgi/content/full/jcb.200712086/DC1).

Effects of EPB41L5 overexpression on E-cadherin localization were examined using TGFβ-untreated epithelial NMuMG

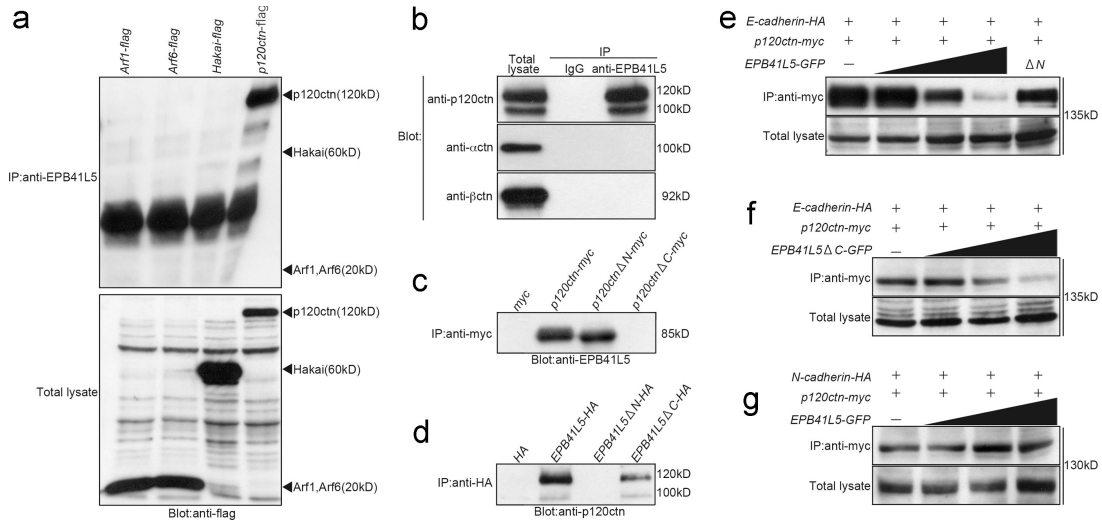

Figure 6. **EPB41L5 interaction with E-cadherin–associated adhesion components.** (a) EPB41L5 binding to Arf1, Arf6, Hakai, and p120 catenin. Each expression vector harboring *Arf1*, *Arf6*, *Hakai*, or *p120 catenin* (*p120ctn*) linked with *flag* was transfected into Cos7 cells 12 h after plating, and the cells were harvested 24 h later. The bottom panel gives the Western blotting for the expression of each transgene in total cell lysates of respective transfectants. In the top panel the lysates were immunoprecipitated with the anti-EPB41L5 antibody, and the presence or absence of each molecule in the immunoprecipitates was blotted with anti-flag antibody. (b) EPB41L5 binding to p120ctn, α-catenin (αctn) and β-catenin (βctn). The left panel gives the expression level of each catenin in TGFβ-treated NMuMG cells. In the other two lanes the cell lysates were immunoprecipitated with rabbit IgG (middle) or rabbit anti-EPB41L5 antibody (right), and the presence of each catenin in the precipitates was blotted with the antibody against each catenin. (c) EPB41L5 binding to p120 catenin. *Myc*, *myc*-linked full-length *p120ctn, myc*-linked *p120ctn* that lacks N-terminal (ΔN), or *myc*-linked *p120ctn* lacking C-terminal armadillo repeats (ΔC) was transfected into Cos7 cells as described in panel a, cell lysates were immunoprecipitated with anti-myc antibody, and the presence or absence of EPB41L5 in the precipitates was blotted with anti-EPB41L5 antibody. (d) p120 catenin binding to EPB41L5. *HA*, *HA*-linked full-length *EPB41L5*, *HA*-linked *EPB41L5* that lacks N-terminal FERM domain (ΔN), or *HA*-linked *EPB41L5* lacking C-terminal (ΔC) was transfected into Cos7 cells, cell lysates were immunoprecipitated with anti-HA antibody, and the presence or absence of p120ctn in the precipitates was blotted with anti-p120ctn antibody. See Fig. 1 A for the site of the *EPB41L5* truncation. (e) Effects of EPB41L5 on the binding between E-cadherin and p120ctn. 1 μg *HA*-linked *E-cadherin* and *myc*-linked p*120ctn* were cotransfected with 0, 1, 2.5, or 5 μg *GFP*-linked full-length *EPB41L5* or with 5 μg *GFP*-linked *EPB41L5* that lacks the N-terminal (ΔN). The bottom panel gives the amount of E-cadherin in total cell lysates. The lysates were immunoprecipitated with anti-myc antibody for p120ctn and the amount of E-cadherin in the precipitates was blotted with anti-HA antibody. (f) Effects of EPB41L5 that lacks C-terminal but retains N-terminal FERM domain on the binding between E-cadherin and p120ctn. (g) Effects of EPB41L5 on the binding between N-cadherin and p120ctn. The binding assay in f and g was conducted as described in panel e.

and T47D cells. The *EPB41L5* overexpression increased the number of E-cadherin–positive vesicles in cytoplasm (Fig. 7, a and d; Fig. S5, b and j), and these vesicles coincided with the Rab5-positive vesicles (Fig. 7, c and d); Rab5-positive vesicles were also enhanced by *EPB41L5* overexpression (Fig. 7 c). EPB41L5 mostly did not colocalize with these vesicles, but might colocalize with the vesicles beneath the membrane (Fig. 7, b and d; Fig. S5, f and j). Furthermore, the overexpression of EPB41L5 that lacked the N-terminal FERM domain did not induce the E-cadherin–positive vesicles (Fig. 7, e–h; Fig. S5, c, g, and k), whereas EPB41L5 with intact N-terminal and lacking the C-terminal (EPB41L5ΔC) did (Fig. 7, i–l; Fig. S5, d, h, and l). Of note is that membrane ruffles and protrusions were enhanced in these epithelial cells overexpressing EPB41L5 (Fig. 7, a–d and i–l; Fig. S5).

EPB41L5 interaction with integrin-associated adhesion components

In TGFβ-treated NMuMG cells endogenous EPB41L5 also bound to β1-integrin and paxillin, but not to FAK, talin, cortactin, or vinculin (Fig. 8 a). Thus, we examined the possibility that EPB41L5 modulates the association between paxillin and integrin, and indeed, EPB41L5 did increase β1-integrin binding to paxillin (Fig. 8 b). The EPB41L5 binding to paxillin occurred through the C terminus of paxillin (Fig. 8 c) and through the C terminus of EPB41L5 (Fig. 8 d). Thus, EPB41L5 interacts with p120ctn through its N terminus and with paxillin through its C terminus. This suggests the possibility that p120ctn is recruited into paxillin complex by EPB41L5. Indeed, in TGFβ-treated NMuMG cells p120ctn associated with paxillin, and this association was abolished by *EPB41L5* siRNA (Fig. 8 e). Furthermore, p120 ctn/paxillin association was enhanced by *EPB41L5* overexpression in NIH3T3 and Cos7 cells (Fig. 8 f).

In NIH3T3- and TGFβ-treated NMuMG cells, EPB41L5 overlapped with paxillin- and α5-integrin–positive focal adhesions (Fig. 9 A; Fig. S5 B, a–d). When EPB41L5 was expressed in epithelial T47D cells, the cells developed remarkable membrane ruffles and protrusions, and the number of paxillin-positive focal adhesions increased dramatically (Fig. 9, Ba and b). EPB41L5 that had N-terminal p120ctn binding domain and lacked the C-terminal paxillin binding domain (EPB41L5ΔC) localized at the plasma membrane, but could not induce membrane ruffles nor enhance focal adhesions (Fig. 9 Bc). On the other hand, EPB41L5 that lacked the N-terminal but had the C-terminal domain (EPB41L5ΔN) did not localize at the plasma membrane but was able to induce membrane ruffles and enhance focal adhesions (Fig. 9 Bd).

As described above, *EPB41L5* siRNA decreased cell attachment to substrate, cell mobility, and cell spreading in NIH3T3 cells (Fig. 5). Normally NIH3T3 cells have paxillin- and α5-integrin–positive focal adhesions where actin fibers terminate,

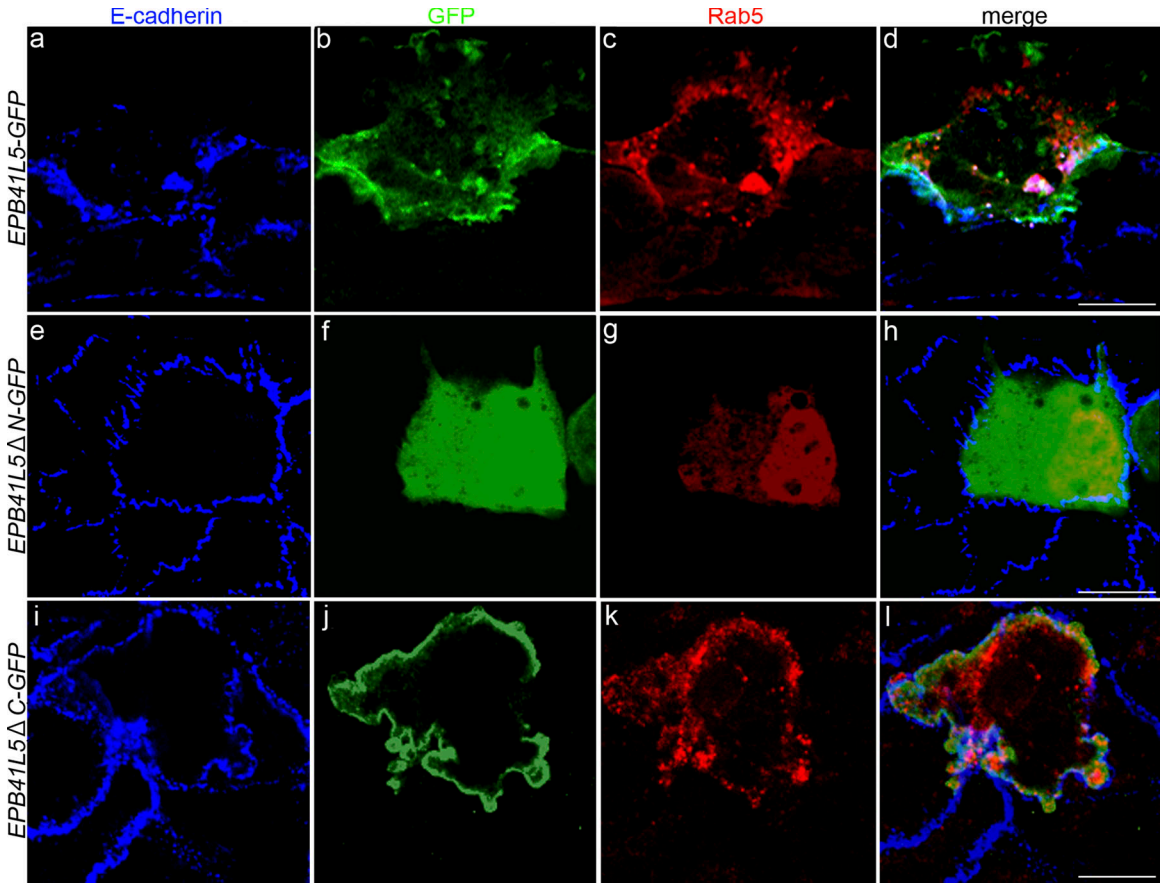

Figure 7. **Effects of EPB41L5 on E-cadherin and Rab5 distribution.** *GFP*-linked full-length *EPB41L5* (a–d), *GFP*-linked *EPB41L5* that lacks N-terminal FERM domain (e–h), or *GFP*-linked *EPB41L5* that lacks C terminus (i–l) was co-transfected with *myc*-linked *Rab5* (to detect endosomes) into epithelial NMuMG cells. (a, e, and i) Endogenous E-cadherin staining (blue), (b, f, and j) GFP staining for EPB41L5 localization (green), (c, g, and k) myc staining for Rab5-positive endosomes (red), and (d, h, and l) merged views. Confluent epithelial NMuMG cells, in the absence of TGFβ, uptake little DNA, and the rare cells that took up DNAs are marked by green and red among most cells that did not (blue). *myc-Rab5* itself has no effect on E-cadherin distribution (e–h) (Palacios et al., 2005). In the NMuMG cells that took up full-length *EPB41L5* (a–d) or *EPB41L5* that lacks C terminus (i–l), the number of E-cadherin–positive vesicles is increased in cytoplasm. The E-cadherin–positive vesicles coincided with Rab5-positive endosomes (d and l); Rab5-positive vesicles are also enhanced. *EPB41L5* that lacks N-terminal FERM domain (e–h) does not increase cytoplasmic E-cadherin–positive vesicles. In each transfection more than 30 GFP-positive cells were examined, all of the cells showing the pattern of EPB41L5, E-cadherin and Rab5 localization shown here. Bars, 30 μm. Similar observations obtained with T47D cells are presented in Fig. S5 A.

being scattered throughout the basal side of the cell body and abundant in filopodia and lamellipodia (Fig. 9, Ca and c). In the *EPB41L5* siRNA-treated NIH3T3 cells α5-integrin–positive structures disappeared (Fig. 9 Cb), and paxillin-positive structures were deformed in the center of the basal side of the cell body, and actin fibers did not terminate in these structures (Fig. 9 Cd). Focal adhesions were also scarce in *EPB41L5* mutant primitive streak cells that crept out in culture (Fig. 9 D).

The above results indicate that EPB41L5 enhances paxillin/integrin interaction and consequently focal adhesion formation. Focal adhesions must dynamically turn over, and their enhancement could be incompatible with active cell movement and spreading as seen in EHD1 (C-terminal Eps15-homology [EH] domain-containing protein) mutants (Jovic et al., 2007). Therefore, FRAP analysis was conducted to examine the effects of EPB41L5 on focal adhesion turnover (Iioka et al., 2007). Paxillin-positive focal adhesions induced in T47D cells by *EPB41L5* overexpression were actively turning over, while *EPB41L5 siRNA* greatly reduced the turnover of paxillin-positive structures in NIH3T3 and TGFβ-treated NMuMG cells (Fig. 9 E; unpublished data).

Discussion

Upon EMT during gastrulation, the down-regulation of cell–cell adhesions must be tightly coordinated with the activation of cell–ECM interaction. EPB41L5 plays critical roles in this coordination, and this study proposes a "displacement" model for its function. EPB41L5 post-transcriptionally destabilizes E-cadherin by binding to p120ctn through its N-terminal FERM domain and reducing the association of p120ctn with E-cadherin. At the same time, EPB41L5 facilitates focal adhesion formation by binding to paxillin through its C-terminal domain and enhancing paxillin association with integrin. The study has revealed a new aspect of the function of band 4.1 superfamily members, which are thought to function as scaffolds for integral membrane proteins.

E-cadherin down-regulation in the EMT during mouse gastrulation is known to be regulated by Fgf signaling; Fgf signaling up-regulates the expression of *Snail*, which acts as a transcriptional repressor inhibiting *E-cadherin* expression (Batlle et al., 2000; Cano et al., 2000). *Fgf8*, *Fgfr1*, or *Snail* mutants

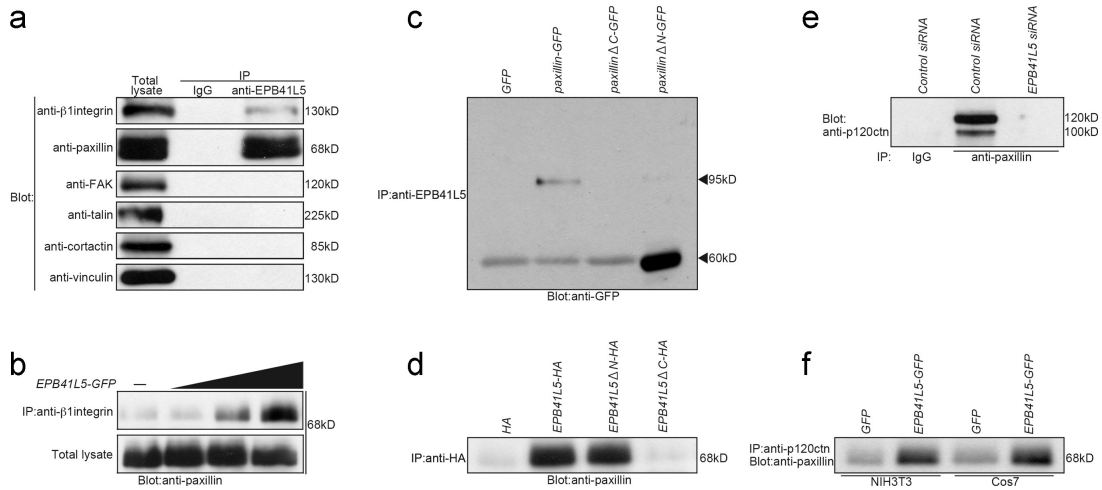

Figure 8. **EPB41L5 interaction with integrin-associated adhesion components.** (a) EPB41L5 binding to integrin-associated adhesion components in TGFβ-treated NMuMG cells. The amount of each component in the total cell lysates is given in the left panel. In the other two lanes the cell lysates were immunoprecipitated with rabbit IgG (middle) or rabbit anti-EPB41L5 antibody (right), and the presence of each component in the precipitates was blotted with the antibody against each molecule indicated at left. (b) Effects of EPB41L5 on the binding between β1-integrin and paxillin. 0, 1, 2.5, or 5 μg *GFP*-linked full-length *EPB41L5* was transfected into Cos7 cells, and the binding assay was performed 24 h later. The bottom panel gives the amount of paxillin in total cell lysates. In the top panel the lysates were immunoprecipitated with anti-β1-integrin antibody, and the amount of paxillin in the precipitates was blotted with anti-paxillin antibody. (c) EPB41L5 binding to paxillin. *GFP*, *GFP*-linked full-length *paxillin, GFP*-linked *paxillin* that lacks C-terminal (ΔC), or *GFP*-linked *paxillin* lacking N-terminal (ΔN) was transfected into Cos7 cells as described in Fig. 6 a, cell lysates were immunoprecipitated with anti-EPB41L5 antibody, and the presence or absence of paxillin in the precipitates was blotted with anti-GFP antibody. (d) Paxillin binding to EPB41L5. *HA*, *HA*-linked full-length *EPB41L5*, *HA*-linked *EPB41L5* that lacks N-terminal FERM domain (ΔN), or *HA*-linked *EPB41L5* lacking C terminus (ΔC) was transfected into Cos7 cells, cell lysates were immunoprecipitated with anti-HA antibody, and the presence or absence of paxillin in the precipitates was blotted with anti-paxillin antibody. See Fig. 1 A for the site of the *EPB41L5* truncation. (e) Effects of EPB41L5 siRNA on p120ctn binding to paxillin. NIH3T3 cells were transfected with control or *EPB41L5* siRNA and harvested 24 h later; cell lysates were immunoprecipitated with rabbit IgG or rabbit anti–mouse paxillin antibody, and the amount of p120ctn in the precipitates was blotted with anti-p120ctn antibody. (f) Effects of EPB41L5 overexpression on p120ctn binding to paxillin. NIH3T3 or Cos7 cells were transfected with *GFP* or *GFP*-linked *EPB41L5*; cell lysates were immunoprecipitated with anti-p120ctn antibody, and paxillin in the precipitates was blotted with anti-paxillin antibody.

fail both to suppress *E-cadherin* and to induce a series of genes of mesoderm development at the transcriptional level (Yamaguchi et al., 1994; Sun et al., 1999; Cano et al., 2000). However, in *EPB41L5* mutants, the expression of *Fgf8*, *Snail*, and other mesodermal markers did occur. At the mRNA level, *E-cadherin* expression was also shut off and *integrin* expression was enhanced. However, at the protein level, E-cadherin persisted and integrin did not appear in *EPB41L5*-deficient invaginating cells at primitive streak and TGFβ-treated NMuMG cells. Thus, EPB41L5 regulates E-cadherin and integrin expression post-transcriptionally. Because E-cadherin was down-regulated at the mRNA level, E-cadherin was eventually depleted in *EPB41L5* mutant mesoderm cells (Fig. 4 c'). On the other hand, α5-integrin was never elevated in the mutant mesoderm cells (Fig. 4 e'). EPB41L5 may stabilize integrin by increasing association with paxillin, and in its absence integrin may be readily degraded, despite the fact that integrin expression is seen at the mRNA level in the mutant mesoderm cells.

Arf6 has been reported to function in both decrease of cell–cell adhesions by E-cadherin degradation and increase in integrin-mediated cell–ECM adhesions (Sabe, 2003). RohA pathway is also known to play key roles in regulation of cell–cell adhesions and cell–ECM adhesions (Kaibuchi et al., 1999; D'Souza-Schorey, 2005). We have made intensive efforts to examine the possibility that EPB41L5 functions in these pathways, but no data have been obtained to suggest such possibility. EPB41L5 does not bind to Arf6 (Fig. 7 A), nor did EPB41L5 affect p120 catenin binding to RhoA or Rac1 (unpublished data). RhoGTPase activity increases with EMT of NMuMG cells by TGFβ; however, *EPB41L5* siRNA did not affect the activities (unpublished data). With the data obtained in this study we have proposed a "displacement" model for EPBL5 functions in cell–cell adhesions and cell–ECM adhesions. However, the possibility that EPBL5 functions in Arf6, RhoA, or another pathway cannot be excluded.

A question in the "replacement" model is why EPBL5 does not affect N-cadherin/p120ctn interaction (Fig. 6 g). Even if EPB41L5 is depleted, N-cadherin expression increases normally in invaginating mesoderm cells and TGFβ-treated NMuMG cells at the protein level (Fig. 4 d'; Fig. 2 Ab). Although the sequences for β-catenin binding sites are highly conserved, those for p120ctn are conserved only moderately between E- and N-cadherins (Kim et al., 2000); it is possible that these cadherins have different affinities to p120ctn. Hakai binds to the p120ctn binding site of E-cadherin, but not to this site of N-cadherin; Hakai degrades E-cadherin but not N-cadherin (Fujita et al., 2002). There is also a report suggesting that an extracellular domain makes N-cadherin different from E-cadherin with respect to functions in EMT and cell–ECM interactions (Kim et al., 2000). This critical issue remains for future studies. Another question is the role of p120ctn in cell–ECM interaction; this study suggests that EPB41L5 recruits p120ctn from E-cadherin–mediated cell–cell adhesions to the integrin/paxillin complex upon EMT. However, the study has not demonstrated any roles of p120ctn in the integrin/paxillin complex for cell–ECM adhesions. This is also an issue worthy of further examination.

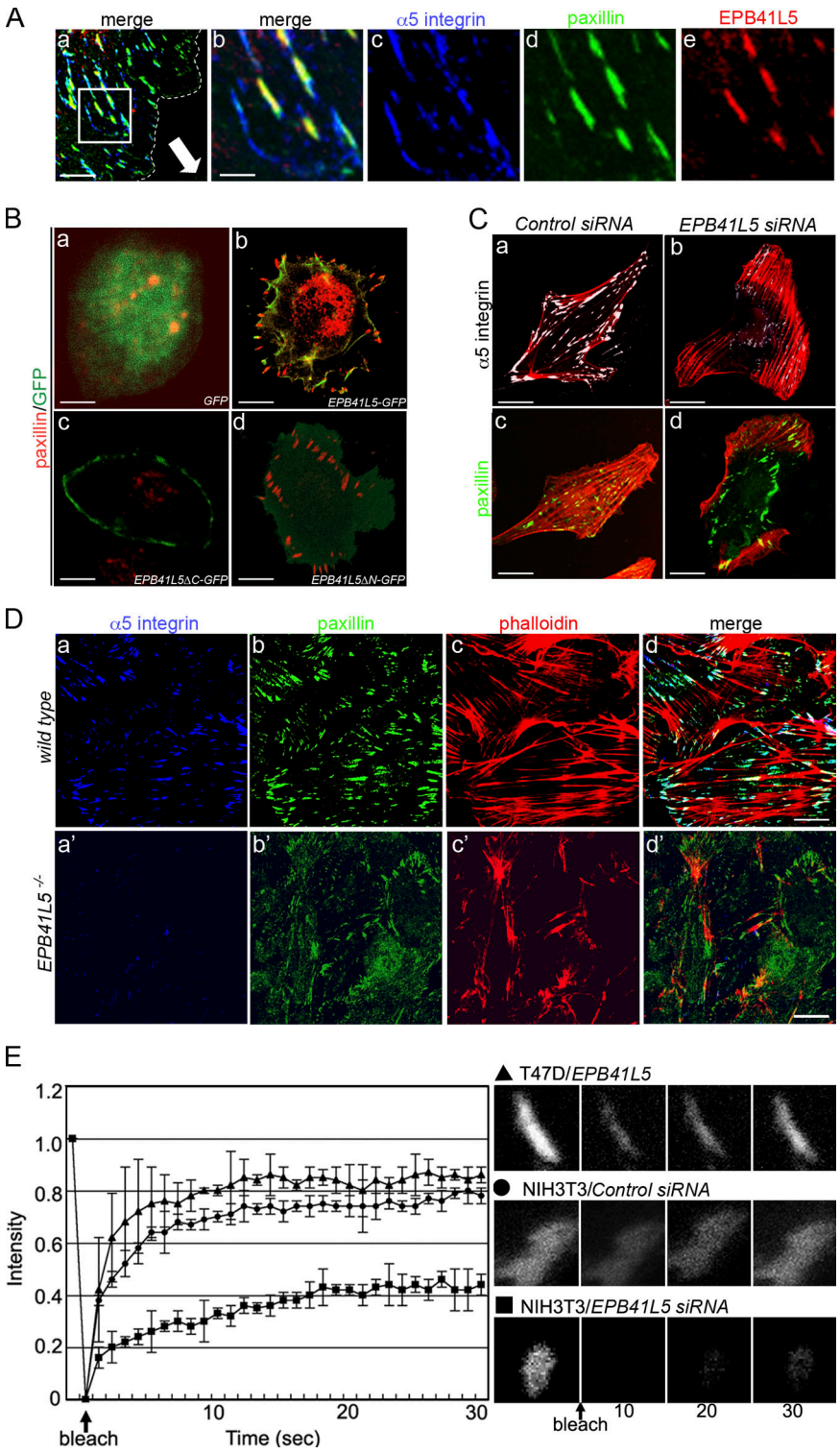

Figure 9. **Effects of EPB41L5 on focal adhesion formation and turnover.** (A) Colocalization of EPB41L5 with α5-integrin and paxillin at the leading edge of NIH3T3 cells. Monolayered NIH3T3 cells were scratched and cultured for 12 h (Fig. 5 Ea); the dotted line indicates the cell periphery, and the direction of the cell movement is indicated by an arrow in panel a. Bars, 10 μm. (b–e) Enlarged views of the boxed area in panel a. (a and b) Merged views of (c) α5-integrin (blue), (d) paxillin (green), and (e) EPB41L5 (red) localization. Bars, 2 μm. Endogenous paxillin and EPB41L5 localization in TGFβ-treated mesenchymal NMuMG cells is also given in Fig. S5 B. (B) Increase in focal adhesions by EPB41L5 expression in T47D cells. *GFP* (a), *GFP*-linked full-length *EPB41L5* (b), *GFP*-linked *EPB41L5* that lacks C-terminal paxillin binding domain (ΔC) (c), or *GFP*-linked *EPB41L5* lacking N-terminal FERM domain (ΔN) (d) was transfected into T47D cells that do not express EPB41L5. The cells are stained for GFP (green) and endogenous paxillin (red). Quantification of paxillin-positive structures is given in Fig. S5 C. Bars, 30 μm. (C) Disappearance of focal adhesions in NIH3T3 cells by *EPB41L5* siRNA. The cells were transfected with control (a and c) or *EPB41L5* siRNA (b and d) and stained for actin (red) and α5-integrin (a and b; white) or paxillin (c and d; green). Bars, 30 μm. (D) Distribution of focal adhesions in wild-type (a–d) and *EPB41L5* mutant (a′–d′) cells. α5-Integrin (a and a′), paxillin (b and b′), and actin (c and c′) expression and merged views (d and d′) are shown on the cells that crept out from the primitive streak cell mass as boxed in Fig. 5, Bb and d. Quantification of paxillin- and α5-integrin–positive structures is given in Fig. S5 D. Bars, 50 μm. (E) FRAP assay. FRAP analysis was conducted with paxillin-GFP expressing T47D cells transfected with *EPB41L5* (▲) or with paxillin-GFP expressing NIH3T3 cells transfected with control (●) or *EPB41L5* siRNA(■). Right panels show examples of fluorescence recovery after photobleaching in the T47D cell overexpressing *EPB41L5* (top), control NIH3T3 cell (middle), and NIH3T3 cells treated with *EPB41L5* siRNA (bottom).

Drosophila Yurt and zebrafish Moe, the members of the EPB41L5 family, are negative regulators of Crb proteins, which control epithelial polarity and apical membrane size in embryonic epithelia and photoreceptor cells (Nelson, 2003; Jensen and Westerfield, 2004; Hsu et al., 2006; Laprise et al., 2006). In mammal EPB41L4b/Ehm2 and EPB41L5/YMO1 are also reported to be able to bind to Crb proteins (Laprise et al., 2006). Furthermore, very recently EPB41L5 has been suggested to function in Crumbs-MPP5 complex for epithelial polarity in MDCK cells (Gosens et al., 2007). However, the defects in the *EPB41L5* mutant ectoderm and endoderm cells were found to include an increase in cell–cell contact, multi-cell stratification, and loss of basement membrane. Defects in cell polarity were not apparent in *EPB41L5* mutant epiblast, neuroectoderm, or endoderm. Electron microscopic observations and marker analysis indicated that tight junction, adherens junction, and desmosome

form normally in *EPB41L5* mutant epithelia. However, the possibility cannot be excluded that EPB41L5 functions in epithelial polarity is complemented by EPB41L4b, another member of the EPB41L5 subfamily, which is also expressed during gastrulation (unpublished data). The increase in cell number, along with multicell stratification, in mutant E7.5 epiblast was not explained by the increase in cell proliferation, nor by the decrease in cell apoptosis; total cell number per embryo was also unchanged. This may also be the case in mutant E8.5 hypertrophic neuroepithelia. It seems likely that the increase in the cell number in epiblast or neuroepithelia is rather brought about by the inhibition of the transition of epiblast or neuroepithelium into mesoderm and endoderm or neural crest cells, respectively.

In vivo, EPB41L5 is not found ubiquitously in epithelial tissues at later stages as it is not in NMuMG or T47D cells. However, EPB41L5 is expressed in the entire embryonic epithelia in ectoderm and endoderm at peri-gastrulation (Fig. S2 B). Why does it not induce EMT there? Some aspects of EMT, such as increase in membrane ruffling and focal adhesions, were induced by EPB41L5 overexpression in epithelial NMuMG and T47D cells. Even in the epithelial monolayer, E-cadherin molecules dynamically turn over by endocytosis and recycling back to the plasma membrane (D'Souza-Schorey, 2005; Xiao et al., 2007). Furthermore, interactions between the epithelial cells and basement membrane are essential to the maintenance of epithelial integrity. In addition, there must exist crosstalk between these cadherin-mediated cell–cell interaction and integrin-mediated cell–ECM interactions even in the epithelium (Sakamoto et al., 2006). EPB41L5 must play roles in these processes in epithelial ectoderm and endoderm, as suggested by the increase in cell adhesion and loss of basement membrane in *EPB41L5* mutant epithelial ectoderm and endoderm cells. However, the output of the EPB41L5-mediated crosstalk is markedly different in epithelial ectoderm and mesenchymal mesoderm. There is no apparent change in the level of the EPB41L5 expression among cells of the three germ layers. It appears probable that EPB41L5 activity is not different in ectoderm and mesoderm cells. In ectoderm, E-cadherin is actively produced, and this may compensate for the E-cadherin destabilization by EPB41L5, whereas in mesoderm cells E-cadherin is not produced at the mRNA level and residual E-cadherin protein in invaginating mesoderm cells may be readily degraded by EPB41L5. In ectoderm, *α5-integrin* is not produced at the mRNA level, and EPB41L5 may be unable to activate focal adhesions, as it can in mesodermal cells which do generate this integrin. However, the possibility remains that an EMT signal activates EPB41L5 by an unknown mechanism.

Recently NIK (NCK-interacting kinase/Map4k4) and p38IP (p38 interacting protein), which function in MAPK cascades, have been reported to down-regulate E-cadherin at the protein level (Xue et al., 2001; Zohn et al., 2006). Movement is inhibited in p38IP mutant mesoderm cells, and this is due to the failure in down-regulation of E-cadherin. EMT during gastrulation is also regulated by Activin/nodal signaling. FLRT3 (fibronectin leucine-rich repeat transmembrane 3) and small GTPase Rnd1 have recently been reported to modulate cell adhesion downstream in this pathway, and independent of FGF signaling, by down-regulating cell surface cadherin through endocytosis (Ogata et al., 2007). However, p38IP and FLRT3/ Rnd1 do not participate in the enhancement of cell–ECM adhesions. In contrast, EPB41L5 not only down-regulates E-cadherin but also activates integrin/paxillin association for cell–ECM interaction.

p120ctn stabilizes E-cadherin at cell–cell contact sites, and its deficiency causes rapid degradation of E-cadherin (Ireton et al., 2002; Davis et al., 2003; Xiao et al., 2007). However, the role of p120ctn has never been suggested in the EMT during gastrulation. Molecular details of how E-cadherin destabilized by EPB41L5 is internalized into endosomes remain for future studies. Paxillin is a key component in focal adhesions, presenting integrin on the cell surface and linking it to the cytoskeleton (Kondo et al., 2000; Hagel et al., 2002). EPB41L5 overexpression facilitated focal adhesion formation in T47D cells, while focal adhesions are deformed in NIH3T3 cells treated with *EPB41L5* siRNA, and scarce in *EPB41L5* mutant cells that emerged from the primitive streak. However, molecular mechanisms how the increase in paxillin/integrin association by EPB41L5 enhances focal adhesion turnover also remains for future studies. The details of post-translational coordination between the down-regulation of cadherin-mediated cell–cell interaction and the increase in integrin-mediated cell–ECM interaction on EMT are largely unknown. The molecular details of how EPB41L5 coordinate these two processes are of particular interest for future study.

Band 4.1 superfamily members are known to maintain epithelial integrity and to be tumor suppressors (Sun et al., 2002). In the ERM family, *merlin* is the gene responsible for neurofibromatosis 2 (Rouleau et al., 1993; Trofatter et al., 1993). DAL-1/Protein 4.1B and Protein 4.1R in the Band 4.1 family are also silenced in non-small cell lung carcinomas, neuroblastomas and other tumors (Tran et al., 1999; Gutmann et al., 2000; Perry et al., 2000; Huang et al., 2001). In contrast, in the EPB41L5 family, mouse *EPB41L4b/Ehm2* was identified as a gene expressed in high-metastatic K1735 murine melanoma cells (Shimizu et al., 2000). The present results are strongly consistent with an oncogenic or metastatic function for EPB41L5.

Materials and methods

Isolation of *EPB41L5*

EPB41L5 was isolated in our efforts to identify *Otx2* targets with the TM library (Murata et al., 2004); the clone in the library is full-length cDNA of 2409 bp.

Plasmids

Arf1-flag, Arf6-flag, Hakai-flag, and p120ctn-flag expression vectors were constructed with pCAGGS-flag vector; E-cadherin-HA, N-cadherin-HA, EPB41L5-HA, EPB41L5ΔC-HA, and EPB41L5ΔN-HA with pCAGGS-HA vector; EPB41L5-GFP, EPB41L5ΔC-GFP, and EPB41L5ΔN-GFP with pEGFP-C1 (Clontech Laboratories, Inc.). p120ctn-myc, p120ctnΔN-myc, p120ctnΔC-myc, paxillin-GFP, paxillin ΔC-GFP, and paxillin ΔN-GFP were prepared previously (Aono et al., 1999; Yano et al., 2004).

Cell culture

NMuMG cells were obtained from American Type Culture Collection (ATCC), and the sources of T47D, NIH3T3, and Cos7 cells are as described (Yano et al., 2004). NIH3T3, Cos7, and whole embryonic cells were cultured in DMEM (Invitrogen) supplemented with 10% FCS; primitive streak was cultured in the same medium as described previously (Zohn et al., 2006). The medium for NMuMG cell culture was further supplemented with 10 μg/ml insulin and cultured as described previously (Miettinen et al., 1994). T47D cells were cultured in RPMI 1640 (Invitrogen) supplemented with 10% FCS. To induce EMT, NMuMG cells were treated with

10 ng/ml TGFβ from 8 h after plating for 48 h. For wound-healing assay, monolayered cells were scratched 12 h after cell plating at a high cell density (Hagel et al., 2002). Cell attachment assay (Oh et al., 1999) and cell aggregation assay (Takeichi, 1977) were performed as described previously. NMuMG, NIH3T3, and T47D cells were transfected with control siRNA (60 nM; Invitrogen), *EPB41L5* siRNA duplexes (60 nM), or each *EPB41L5 DNA* (5 μg unless otherwise indicated) using Lipofectoamine2000 (Invitrogen) in Opti-MEM (Invitrogen) at the time of cell seeding, according to the manufacturer's instructions. *EPB41L5* siRNA duplexes used are 5′-CAGCACAACACAACCUGAAGAUCUU-3′ and 5′-AAGAUCUUCAGGUUGUGUUGUGCUG-3′. Cos7 cells were transfected with DNAs (5 μg unless otherwise indicated) using Polyfect Transfection Reagent (QIAGEN) at 12 h after plating and assayed after another 24-h culture.

Construction of targeting vector

A BAC clone, RP23-443K20, which contains the translational start site of the *EPB41L5* gene was obtained from BACPAC Resources (http://bacpac.chori.org/), and targeting and control vectors were constructed as described previously (Murata et al., 2004). Primers used were the 37-bp pI (5′-CAGAAAGGTTACTAGTTGAGACTCTGGTGAGATCAGG-3′) and 26-bp pII (5′-AACTCACCGGGACTATAGGGGTCACC-3′) sequences to amplify the 5.3-kb 5′ arm of the targeting vector, the 25-bp pIII (5′-GACCCACTCGCTAGCTGCCATCTGC-3′) and 37-bp pIV (5′-GACTGGCCTGCATCACCTCCAACAGCCAGAACTTACG-3′) sequences to amplify the 4kb 3′ arm of the targeting vector, and pIII and pV (5′-GCCAAGCCTGCATCAACTCCAACAGTTAGCAATTACC-3′) to amplify the 4.8-kb 3′ arm of the control vector. Their locations are indicated in Fig. S1 A. The six underlined nucleotides in pI, pIV, and pV sequences were converted into AscI and XhoI recognition sequences, GTCGAC and CTCGAG, respectively, to generate each primer. The amplified products were digested by each restriction enzyme: AscI and NotI for the 5.3-kb 5′ arm, SpeI and XhoI for the 4-kb 3′ arm, and SpeI and NotI for the 4.8-kb 3′ arm, respectively. To construct the targeting vector, the 5′ 5.3-kb and 3′ 4-kb arms were inserted into the AscI/NotI sites and NheI/XhoI sites of 5′ and 3′ cloning sites, respectively, of the *LacZ/Neo-DTA* vector (Murata et al., 2004). To construct the control vector, the 3′ 4.8-kb arm was inserted into the SpeI/NotI sites of the 3′ cloning site of the *LacZ/Neo* vector. In the targeting vector and thus in the homologous recombinant a 2.4-kb region between pII and pIII sequences was replaced with the *LacZ/Neo* cassette.

Generation and housing of *EPB41L5* mutant mice

Homologous recombinant ES cells were isolated, and *EPB41L5* mutant mice (accession no. CDB0032K; http://www.cdb.riken.jp/arg/mutant%20mice%20list.html) were generated as described previously (Murata et al., 2004). Mice were housed in an environmentally controlled room following the CDB guidelines for animal experiments.

Genotyping and phenotyping of mice

Southern hybridization was performed with 3′ and 5′ probes located outside of the regions used in the targeting vector (Fig. S1 A) as well as the *neo* probe as described previously (Murata et al., 2004). Genotypes of mice and embryos were determined routinely by PCR with genomic DNAs from tails or yolk sacs. Primers used were p3 (5′-GGACGGTACAGATGTCAGTGTGG-3′) and p4 (5′-CTGTACTCCCACATT GGCAGC-3′) to detect wild-type allele and p5 (5′-GAATGG AAGGATTGG AGCTACGG-3′) and p4 to detect mutant allele; their locations are indicated in Fig. S1 A. Histological analysis was performed as described previously (Murata et al., 2004).

RT-PCR analysis

1 μg of total RNAs from E8.5 brain was subjected to RT-PCR analysis. The cDNA synthesis was performed using ReverTra-Plus (TOYOBO), following the protocol provided by the manufacturer. The purity and the quantity of the cDNAs were analyzed with GAPDH-specific primers: GAPDH-sense (5′-TGTCATCAACGGGAAGCCCA-3′)andGAPDH-antisense(5′-TTGTCATGGATGACCTTGGC-3′). Primers used to detect *EPB41L5* transcripts were: R1 (5′-GGCCTCTGCAGACTGGGACTCC-3′), R2 (5′-GGTGACCGCCGAGAGGCCAAGC-3′), R3 (5′-AGCTGAGGAGGTTTCTGTCCAG-3′), R4 (5′-TTCCCCCGGCTAGGCTTAGAGG-3′), F (ACCATCCTGACGTCCACCCCAG), and R (GTGGTGCTGGTGCTGATG CTGG); the locations of each primer are indicated in Fig. S1 A and Fig. 1 Aa. The amplification conditions were: pretreatment, 2 min at 94°C; PCR, 25 cycles (denaturation, 15 s at 95°C; annealing, 30 s at 58°C; extension, 90 s at 72°C); post-treatment, 7 min at 72°C. The sizes of PCR products were 350 bp with the R1/R2, 500 bp with the R3/R4, 214bp with F/R, and 305 bp with GAPDH-sense/antisense primer sets, respectively.

RNA in situ hybridization analysis

The probe to detect *EPB41L5* was a 970-bp fragment corresponding to its 3′ part (596–731 aa). Probes to detect *Brachyury* and *Snail* are as described previously (Herrmann, 1991; Smith et al., 1992). Embryos were processed as described previously for in situ hybridization (Murata et al., 2004).

Electron microscopic analysis

Transmission electron microscopic analysis was conducted as described previously (Yonemura et al., 2002). In brief, samples were fixed with 2.5% glutaraldehyde, 2% formaldehyde in 0.1 M cacodylate buffer (pH 7.4) for 2 h at room temperature followed by postfixation with 1% OsO_4 in the same buffer for 2 h on ice. The samples were rinsed with distilled water, stained with 0.5% aqueous uranyl acetate for 2 h at room temperature, dehydrated with ethanol, and embedded in Polybed 812 (Polyscience). Ultrathin sections were cut using an ultramicrotome (Ultracut; Leica), doubly stained with uranyl acetate and lead citrate and observed at 80 kV accelerating voltage using a transmission electron microscope (JEM 1010; JEOL), equipped with a CCD camera (model 2k; Hamamatsu Photonics). Images were processed with Photoshop CS software (Adobe).

Immunohistology and immunoblotting

Polyclonal mouse and rabbit anti–mouse EPB41L5 antibodies were raised against 623–731 amino acids at the C terminus (Fig. 1 Aa). The other primary antibodies used were rabbit anti–mouse type IV collagen (LSL), rabbit anti–mouse laminin (Harbor Bio-Products), mouse anti–mouse N-cadherin (BD Biosciences), rat anti–mouse α5-integrin (BD Biosciences), mouse anti–mouse β1-integrin (BD Biosciences), mouse monoclonal anti–mouse α-catenin (Sigma-Aldrich), mouse monoclonal anti–mouse β-catenin (Sigma-Aldrich), mouse anti–mouse p120ctn (BD Biosciences), mouse anti–mouse paxillin (BD Biosciences), mouse anti–mouse FAK (Millipore), mouse anti–mouse talin (Invitrogen), rabbit anti–mouse cortactin (Cell Signaling Technology), mouse anti–mouse vinculin (Millipore), mouse monoclonal anti–mouse β-actin (clone AC-15; Sigma-Aldrich), mouse monoclonal anti-flag (Sigma-Aldrich), mouse monoclonal anti-HA (clone HA-7; Sigma-Aldrich), mouse monoclonal anti-myc (Sigma-Aldrich), and rabbit polyclonal anti-GFP (MBL International).

The anti–E-cadherin antibody used for its effect on the migration of primitive streak cells in Fig. 5 B is rat monoclonal anti-uvomorulin/E-cadherin antibody (Sigma-Aldrich), and that used in other studies in Fig. 1 B; Fig. 2, Ab and Bb; Fig. 4; Fig. 7; and Fig. S5 is rat anti–mouse E-cadherin antibody (Shimamura and Takeichi, 1992). AlexaFluor 488–, 594–, or 647–conjugated secondary antibodies and mouse IgG were obtained from Invitrogen.

Immunohistology was performed as described previously (Yano et al., 2004). In brief, cells were fixed in 4% paraformaldehyde for 10 min at room temperature and permeabilized with 0.1% Triton X-100 for 5 min at room temperature. Blocking was performed with 3% BSA (Sigma-Aldrich) in PBS at room temperature for 1 h. The cells were incubated with primary antibody properly diluted with the blocking solution at room temperature for 1 h, and subsequently with the secondary antibody for 1 h at room temperature. Samples were mounted in Vectorshield (Vector Labratories). Images were analyzed using a laser scanning confocal microscope (LSM510) mounted on an inverted microscope (Axiovert 100M), using Plan-Neofluar 40×/1.30 NA and Plan-Apochromat 63×/1.30 NA objectives (Carl Zeiss, Inc.). Images were processed with Photoshop CS software (Adobe). Western blot analysis and immunoprecipitation assay were conducted as described previously (Yano et al., 2004).

FRAP analysis

Paxillin-GFP transgene directed by CMV promoter was prepared with pEGFP-C1 (Clontech Laboratories, Inc.), and NIH3T3 and T47D cell lines permanently expressing the transgene were established. These cell lines were transfected with control or *EPB41L5* siRNA or with *EPB41L5* expression vector, and FRAP assay was conducted as described previously (Iioka et al., 2007).

Online supplemental material

Fig. S1 shows the targeted disruption of the *EPB41L5* gene. Fig. S2 shows *EPB41L5* expression in vivo and mutant phenotype. Fig. S3 shows marker analyses of *EPB41L5* mutant phenotype by RNA in situ hybridization. Fig. S4 shows the roles of EPB41L5 in cell–substrate interaction by the assay with TGFβ-treated NMuMG cells. Fig. S5 shows the roles of EPB41L5 in cell–cell and cell–substrate adhesions (E-cadherin distribution in T47D cells, EPB41L5 and paxillin localization in mesenchymal NMuMG cells, and focal adhesion formation in T47D cells and mutant cells). Online supplemental material is available at http://www.jcb.org/cgi/content/full/jcb.200712086/DC1.

We thank Dr. M. Takeichi for critical discussion, the Laboratory of Animal Resources and Genetic Engineering (CDB) for generation and housing of the mutant mice, Ms. K. Misaki for technical assistance in electron microscopic analyses, and Dr. T. Murata for his technical advice. We are also grateful to those who kindly gave us probes for RNA in situ hybridization and antibodies.

This study was supported by a Grant-in-Aid for Creative Scientific Research from the Japan Society for the Promotion of Science.

Submitted: 17 December 2007
Accepted: 25 August 2008

References

Aono, S., S. Nakagawa, A.B. Reynolds, and M. Takeichi. 1999. p120(ctn) acts an inhibitory regulator of cadherin function in colon carcinoma cells. *J. Cell Biol.* 145:551–562.

Batlle, E., E. Sancho, C. Franci, D. Dominguez, M. Monfar, J. Baulida, and A. Garcia de Herreros. 2000. The transcription factor snail is a repressor of E-cadherin gene expression in epithelial tumour cells. *Nat. Cell Biol.* 2:84–89.

Cano, A., M.A. Perez-Moreno, I. Rodrigo, A. Locascio, M.J. Blanco, M.G. del Barrio, F. Portillo, and M.A. Nieto. 2000. The transcription factor snail controls epithelial-mesenchymal transitions by repressing E-cadherin expression. *Nat. Cell Biol.* 2:76–83.

Carver, E.A., R. Jiang, Y. Lan, K.F. Oram, and T. Gridley. 2001. The mouse snail gene encodes a key regulator of the epithelial-mesenchymal transition. *Mol. Cell. Biol.* 21:8184–8188.

Davis, M.A., R.C. Ireton, and A.B. Reynolds. 2003. A core function for p120-catenin in cadherin turnover. *J. Cell Biol.* 163:525–534.

D'Souza-Schorey, C. 2005. Disassembling adherens junctions: breaking up is hard to do. *Trends Cell Biol.* 15:19–26.

Fujita, Y., G. Krause, M. Scheffner, D. Zechner, H.E. Leddy, J. Behrens, T. Sommer, and W. Birchmeier. 2002. Hakai, a c-Cbl-like protein, ubiquitinates and induces endocytosis of the E-cadherin complex. *Nat. Cell Biol.* 4:222–231.

Gosens, I., A. Sessa, A.I. den Hollander, S.J. Letteboer, V. Belloni, M.L. Arends, A. Le Bivic, F.P. Cremers, V. Broccoli, and R. Roepman. 2007. FERM protein EPB41L5 is a novel member of the mammalian CRB-MPP5 polarity complex. *Exp. Cell Res.* 313:3959–3970.

Gutmann, D.H., J. Donahoe, A. Perry, N. Lemke, K. Gorse, K. Kittiniyom, S.A. Rempel, J.A. Gutierrez, and I.F. Newsham. 2000. Loss of DAL-1, a protein 4.1-related tumor suppressor, is an important early event in the pathogenesis of meningiomas. *Hum. Mol. Genet.* 9:1495–1500.

Hagel, M., E.L. George, A. Kim, R. Tamimi, S.L. Optiz, C.E. Turner, A. Imamoto, and S.M. Thomas. 2002. The adaptor protein paxillin is essential for normal development in the mouse and is a critical transducer of fibronectin signaling. *Mol. Cell. Biol.* 22:901–915.

Herrmann, B.G. 1991. Expression pattern of the Brachyury gene in whole-mount TWis/TWis mutant embryos. *Development*. 113:913–917.

Hsu, Y.C., J.J. Willoughby, A.K. Christensen, and A.M. Jensen. 2006. Mosaic Eyes is a novel component of the Crumbs complex and negatively regulates photoreceptor apical size. *Development.* 133:4849–4859.

Huang, S., U.D. Lichtenauer, S. Pack, C. Wang, A.C. Kim, M. Lutchman, C.A. Koch, J. Torres-Cruz, S.C. Huang, E.J. Jr. Benz, et al. 2001. Reassignment of the EPB4.1 gene to 1p36 and assessment of its involvement in neuroblastomas. *Eur. J. Clin. Invest.* 31:907–914.

Iioka, H., S. Iemura, T. Natsume, and N. Kinoshita. 2007. Wnt signalling regulates paxillin ubiquitination essential for mesodermal cell motility. *Nat. Cell Biol.* 9:813–821.

Ireton, R.C., M.A. Davis, J. van Hengel, D.J. Mariner, K. Barnes, M.A. Thoreson, P.Z. Anastasiadis, L. Matrisian, L.M. Bundy, L. Sealy, et al. 2002. A novel role for p120 catenin in E-cadherin function. *J. Cell Biol.* 159:465–476.

Jensen, A.M., and M. Westerfield. 2004. Zebrafish mosaic eyes is a novel FERM protein required for retinal lamination and retinal pigmented epithelial tight junction formation. *Curr. Biol.* 14:711–717.

Jovic, M., N. Naslavsky, D. Rapaport, M. Horowitz, and S. Caplan. 2007. EHD1 regulates beta1 integrin endosomal transport: effects on focal adhesions, cell spreading and migration. *J. Cell Sci.* 120:802–814.

Kaibuchi, K., S. Kuroda, and M. Amano. 1999. Regulation of the cytoskeleton and cell adhesion by the Rho family GTPases in mammalian cells. *Annu. Rev. Biochem.* 68:459–486.

Kim, J.B., S. Islam, Y.J. Kim, R.S. Prudoff, K.M. Sass, M.J. Wheelock, and K.R. Johnson. 2000. N-cadherin extracellular repeat 4 mediates epithelial to mesenchymal transition and increased motility. *J. Cell Biol.* 151:1193–1206.

Kondo, A., S. Hashimoto, H. Yano, K. Nagayama, Y. Mazaki, and H. Sabe. 2000. A new paxillin-binding protein, PAG3/Papalpha/KIAA0400, bearing an ADP-ribosylation factor GTPase-activating protein activity, is involved in paxillin recruitment to focal adhesions and cell migration. *Mol. Biol. Cell.* 11:1315–1327.

Laprise, P., S. Beronja, N.F. Silva-Gagliardi, M. Pellikka, A.M. Jensen, C.J. McGlade, and U. Tepass. 2006. The FERM protein Yurt is a negative regulatory component of the Crumbs complex that controls epithelial polarity and apical membrane size. *Dev. Cell.* 11:363–374.

Lee, J.D., N.F. Silva-Gagliardi, U. Tepass, C.J. McGlade, and K.V. Anderson. 2007. The FERM protein Epb4.1l5 is required for organization of the neural plate and for the epithelial-mesenchymal transition at the primitive streak of the mouse embryo. *Development.* 134:2007–2016.

Lee, J.M., S. Dedhar, R. Kalluri, and E.W. Thompson. 2006. The epithelial-mesenchymal transition: new insights in signaling, development, and disease. *J. Cell Biol.* 172:973–981.

Miettinen, P.J., R. Ebner, A.R. Lopez, and R. Derynck. 1994. TGF-beta induced transdifferentiation of mammary epithelial cells to mesenchymal cells: involvement of type I receptors. *J. Cell Biol.* 127:2021–2036.

Mitra, S.K., D.A. Hanson, and D.D. Schlaepfer. 2005. Focal adhesion kinase: in command and control of cell motility. *Nat. Rev. Mol. Cell Biol.* 6:56–68.

Murata, T., K. Furushima, M. Hirano, H. Kiyonari, M. Nakamura, Y. Suda, and S. Aizawa. 2004. ang is a novel gene expressed in early neuroectoderm, but its null mutant exhibits no obvious phenotype. *Gene Expr. Patterns.* 5:171–178.

Nelson, W.J. 2003. Adaptation of core mechanisms to generate cell polarity. *Nature.* 422:766–774.

Ogata, S., J. Morokuma, T. Hayata, G. Kolle, C. Niehrs, N. Ueno, and K.W. Cho. 2007. TGF-beta signalling-mediated morphogenesis: modulation of cell adhesion via cadherin endocytosis. *Genes Dev.* 21:1817–1831.

Oh, E.S., H. Gu, T.M. Saxton, J.F. Timms, S. Hausdorff, E.U. Frevert, B.B. Kahn, T. Pawson, B.G. Neel, and S.M. Thomas. 1999. Regulation of early events in integrin signaling by protein tyrosine phosphatase SHP-2. *Mol. Cell. Biol.* 19:3205–3215.

Palacios, F., J.S. Tushir, Y. Fujita, and C. D'Souza-Schorey. 2005. Lysosomal targeting of E-cadherin: a unique mechanism for the down-regulation of cell adhesion during epithelial to mesenchymal transition. *Mol. Cell. Biol.* 25:389–402.

Peifer, M., and A.S. Yap. 2003. Traffic control: p120-catenin acts as a gatekeeper to control the fate of classical cadherins in mammalian cells. *J. Cell Biol.* 163:437–440.

Perry, A., D.X. Cai, B.W. Scheithauer, P.E. Swanson, C.M. Lohse, I.F. Newsham, A. Weaver, and D.H. Gutmann. 2000. Merlin, DAL-1, and progesterone receptor expression in clinicopathologic subsets of meningioma: a correlative immunohistochemical study of 175 cases. *J. Neuropathol. Exp. Neurol.* 59:872–879.

Rouleau, G.A., P. Merel, M. Lutchman, M. Sanson, J. Zucman, C. Marineau, K. Hoang-Xuan, S. Demczuk, C. Desmaze, B. Plougastel, et al. 1993. Alteration in a new gene encoding a putative membrane-organizing protein causes neuro-fibromatosis type 2. *Nature.* 363:515–521.

Sabe, H. 2003. Requirement for Arf6 in cell adhesion, migration, and cancer cell invasion. *J. Biochem.* 134:485–489.

Sakamoto, Y., H. Ogita, T. Hirota, T. Kawakatsu, T. Fukuyama, M. Yasumi, N. Kanzaki, M. Ozaki, and Y. Takai. 2006. Interaction of integrin alpha(v)beta3 with nectin. Implication in cross-talk between cell-matrix and cell-cell junctions. *J. Biol. Chem.* 281:19631–19644.

Shimamura, K., and M. Takeichi. 1992. Local and transient expression of E-cadherin involved in mouse embryonic brain morphogenesis. *Development.* 116:1011–1019.

Shimizu, K., Y. Nagamachi, M. Tani, K. Kimura, T. Shiroishi, S. Wakana, and J. Yokota. 2000. Molecular cloning of a novel NF2/ERM/4.1 superfamily gene, ehm2, that is expressed in high-metastatic K1735 murine melanoma cells. *Genomics.* 65:113–120.

Smith, D.E., F. Franco del Amo, and T. Gridley. 1992. Isolation of Sna, a mouse gene homologous to the Drosophila genes snail and escargot: its expression pattern suggests multiple roles during postimplantation development. *Development.* 116:1033–1039.

Sun, C.X., V.A. Robb, and D.H. Gutmann. 2002. Protein 4.1 tumor suppressors: getting a FERM grip on growth regulation. *J. Cell Sci.* 115:3991–4000.

Sun, X., E.N. Meyers, M. Lewandoski, and G.R. Martin. 1999. Targeted disruption of Fgf8 causes failure of cell migration in the gastrulating mouse embryo. *Genes Dev.* 13:1834–1846.

Takeichi, M. 1977. Functional correlation between cell adhesive properties and some cell surface proteins. *J. Cell Biol.* 75:464–474.

Tran, Y.K., O. Bogler, K.M. Gorse, I. Wieland, M.R. Green, and I.F. Newsham. 1999. A novel member of the NF2/ERM/4.1 superfamily with growth suppressing properties in lung cancer. *Cancer Res.* 59:35–43.

Trofatter, J.A., M.M. MacCollin, J.L. Rutter, J.R. Murrell, M.P. Duyao, D.M. Parry, R. Eldridge, N. Kley, A.G. Menon, K. Pulaski, et al. 1993. A novel moesin-, ezrin-, radixin-like gene is a candidate for the neurofibromatosis 2 tumor suppressor. *Cell.* 72:791–800.

Yamaguchi, T.P., K. Harpal, M. Henkemeyer, and J. Rossant. 1994. fgfr-1 is required for embryonic growth and mesodermal patterning during mouse gastrulation. *Genes Dev.* 8:3032–3044.

Yano, H., Y. Mazaki, K. Kurokawa, S.K. Hanks, M. Matsuda, and H. Sabe. 2004. Roles played by a subset of integrin signaling molecules in cadherin-based cell-cell adhesion. *J. Cell Biol.* 166:283–295.

Yonemura, S., T. Matsui, S. Tsukita, and S. Tsukita. 2002. Rho-dependent and -independent activation mechanisms of ezrin/radixin/moesin proteins: an essential role for polyphosphoinositides in vivo. *J. Cell Sci.* 115:2569–2580.

Xiao, K., R.G. Oas, C.M. Chiasson, and A.P. Kowalczyk. 2007. Role of p120-catenin in cadherin trafficking. *Biochim. Biophys. Acta.* 1773:8–16.

Xue, Y., X. Wang, Z. Li, N. Gotoh, D. Chapman, and E.Y. Skolnik. 2001. Mesodermal patterning defect in mice lacking the Ste20 NCK interacting kinase (NIK). *Development.* 128:1559–1572.

Zohn, I.E., Y. Li, E.Y. Skolnik, K.V. Anderson, J. Han, and L. Niswander. 2006. p38 and a p38-interacting protein are critical for downregulation of E-cadherin during mouse gastrulation. *Cell.* 125:957–969.